UNIVERSITÀ POLITECNICA DELLE MARCHE
Repository ISTITUZIONALE

On the use of Lagrange Multiplier State-Space Substructuring in dynamic substructuring analysis

This is the peer reviewd version of the followng article:

Original
On the use of Lagrange Multiplier State-Space Substructuring in dynamic substructuring analysis / Dias, Rso; Martarelli, M; Chiariotti, P. - In: MECHANICAL SYSTEMS AND SIGNAL PROCESSING. - ISSN 0888-3270. - 180:(2022). [10.1016/j.ymssp.2022.109419]

Availability:
This version is available at: 11566/315592 since: 2024-03-29T07:31:06Z

Publisher:

Published
DOI:10.1016/j.ymssp.2022.109419

Terms of use:

The terms and conditions for the reuse of this version of the manuscript are specified in the publishing policy. The use of copyrighted works requires the consent of the rights' holder (author or publisher). Works made available under a Creative Commons license or a Publisher's custom-made license can be used according to the terms and conditions contained therein. See editor's website for further information and terms and conditions.
This item was downloaded from IRIS Università Politecnica delle Marche (https://iris.univpm.it). When citing, please refer to the published version.

(Article begins on next page)

26 December 2024

Highlights

Performing Dynamic Substructuring analysis with Lagrange Multiplier State-Space Substructuring

R.S.O. Dias, M. Martarelli, P. Chiariotti

- LM-SSS is reliable to couple/decouple SSMs estimated from measured FRFs.
- UCF performs similarly to the coupling forms available in literature.
- UCF avoids the computation of multiple nullspaces and the selection of subspaces.
- The coupled SSMs minimal form is found by using tailored post-processing procedures.
- The unique set of DOFs can be retained by using a Boolean localization matrix.

Performing Dynamic Substructuring analysis with Lagrange Multiplier State-Space Substructuring

R.S.O. Dias[a,*], M. Martarelli[a], P. Chiariotti[b]

[a]*Department of Industrial Engineering and Mathematical Sciences, Università Politecnica delle Marche, Via Brecce Bianche, Ancona, 60131, Marche, Italy*
[b]*Department of Mechanical Engineering, Politecnico di Milano, Via Privata Giuseppe La Masa, Milan, 20156, Lombardia, Italy*

Abstract

In this article, the formulation of Lagrange Multiplier State-Space Substructuring (LM-SSS) is presented and extended to directly compute coupled displacement and velocity state-space models. The LM-SSS method is applied to couple and decouple state-space models established in the modal domain. Moreover, it is used together with tailored post-processing procedures to eliminate the redundant states originated from the coupling and decoupling operations. This specific formulation of the LM-SSS approach made it possible to develop a tailored coupling form, named Unconstrained Coupling Form (UCF). UCF just requires the computation of a nullspace and does not rely on the selection of a subspace from a nullspace. An explanation of all the steps in order to compute state-space models without redundant states originated from the coupling and decoupling procedures is also given. LM-SSS was compared with the Lagrange Multiplier Frequency Based Substructuring (LM-FBS) approach, which is currently widely recognized as a reference approach. This was done both in terms of: a) coupled FRFs derived by coupling the state-space models of two substructures and b) decoupled FRFs derived by decoupling the state-space model of a component from the coupled model. As for the first validation, LM-SSS showed to be suitable to compute minimal order coupled models and UCF turned out to have similar performance as other coupling forms already presented to the scientific community. As for the decoupling task, the FRFs derived from the LM-SSS approach turned out to perfectly match those obtained by LM-FBS. Moreover, it was also demonstrated that the elimination of the redundant states originated from the decoupling operation was correctly performed.

Keywords: Dynamic Substructuring, State-Space Substructuring, Lagrange Multiplier State-Space Substructuring, Unconstrained Coupling Form, State-Space Models

1. Introduction

Dynamic Substructuring (DS) was introduced in the last century with the belief that complex structures can be analyzed in a more efficient way if they are considered as assemblies of several simpler components. From its first introduction, this idea pushed the scientific community to an intense activity in this field, and several DS approaches have been released [1]. Examples of those techniques are the ones clustered under the labels Component Mode Synthesis (CMS) and Frequency Based Substructuring (FBS). In the CMS techniques (see, for instance [2] and [3]), the substructures are usually represented in modal domain by using a set of modes (which might include static, quasi-static and vibration modes depending on the CMS method [4]). These methods found many applications when a DS analysis is intended to be performed with numerical data.

In the FBS methods, the components are characterized by their Frequency Response Functions (FRFs). For this reason, FBS methods are typically used with experimental data. Examples of FBS techniques developed can be found, for instance, in [5] and [6]. In [7], a new DS technique denominated Impulse Based Substructuring (IBS) is

*Corresponding author.
Email addresses: r.dasilva@staff.univpm.it (R.S.O. Dias), m.martarelli@staff.univpm.it (M. Martarelli), paolo.chiariotti@polimi.it (P. Chiariotti)

discussed. This technique describes the substructures by using Impulse Response Functions (IRF). Hence, IBS uses a time domain formulation with respect to FBS for performing DS.

Another group of DS methods is the one named State-Space Substructuring (SSS). In SSS techniques the components are represented by state-space models. These methods are suitable to deal with both numerical and experimental data. The approach discussed in this paper belongs to this group of methods.

One of the first SSS techniques was developed by Su and Juang in [8]. Their approach will be referred from now on as "classical SSS". The implementation of this method relies on the construction of an uncoupled state-space model by writing the state-space models of the substructures in a block diagonal form. Afterwards, a coupling matrix is defined and used to enforce the coupling conditions (compatibility and equilibrium) on this diagonal uncoupled model in order to obtain the coupled state-space model. This method is simple to understand, being also able to couple several structures at same time. Nevertheless, it has some important limitations. Firstly, it requires the inversion of two different matrices to compute the coupled state-space model, secondly it is unable to compute minimal-order coupled state-space models. This means that the computed coupled state-space model will contain redundant states. The presence of such states does not affect the quality of the input-output transfer functions that can be computed from the coupled state-space model [8]. However, by computing a minimal-order state-space model the number of states is reduced and consequently the computational effort required in calculations with the coupled state-space model will be also reduced. On the one hand, this minimal-order representation paves the way to the use of these approaches for Hardware-in-the-loop applications (e.g. real-time substructuring), on the other hand, it turns out to be a more elegant representation of the problem.

As we eliminate one DOF for each pair of connected DOFs, one state and its respective first order derivate must also be eliminated to avoid the presence of redundant states [8]. Hence, the minimal-order state-space model will always present $n - 2n_J$ states (being n the sum of the number of states of the coupled state-space models and n_J the number of interface outputs). If the coupling is performed with state-space models written in physical coordinates (for which the physical meaning of the states and outputs is the same), the states, which initially represented matching interface outputs, are representative of the correspondent coupled interface output (the same is valid for the respective first order derivatives). Hence, they represent the same physical quantity. However, the computation of the minimal-order coupled model cannot be performed by simply keeping on the coupled model just one state from each group of states (whose physical meaning is the same), because each of these states has a non-negligible contribution for the state-space model. Therefore, this state elimination must guarantee that the contribution of the states to be eliminated is retrieved by the one that is kept on the model. To properly perform the elimination of the redundant states, one can follow the post-processing procedures described in [9].

When working with state-space models estimated from measured data, these models are usually obtained in modal domain. Hence, it is difficult to say which states correspond to matching interface outputs, turning the elimination of the redundant states infeasible. On the other hand, as pointed out by Gibanica et al. in [10],[11], a transformation of a state-space model written in modal coordinates into physical ones is not suitable for experimental models. In general, for these models $n >> n_o$ (being n_o the number of outputs), hence this transformation would impose a tremendous constraint on the model in order to force it to have as many states as two times the number of outputs.

A solution to obtain minimal-order coupled state-space models was outlined by Sjövall and Abrahamsson in [12]. They suggested to partially transform the state vector of the state-space models of the substructures into physical domain before coupling them. This transformation was denominated as coupling form being enforced by applying a similarity state vector transformation as described in [12]. By performing this procedure, the state vector of the state-space models will be composed by the first derivate of the interface outputs, by the interface outputs and $n - 2n_J$ internal states.

When the state-space models to be coupled are transformed into this coupling form, their state-space matrices present a particular structure, for which the first block row of the state equation is representative of a second order differential equation, making it possible to perform coupling by directly summing those block rows [10],[13]. This coupling procedure is possible, because the applied similarity transformation guarantees that the contribution of the interface inputs to the response of the internal states is null. Therefore, the internal states remain uncoupled and are just correctly placed on the coupled state-space model [10]. This SSS technique is able to mitigate the problems of classical SSS, since the coupling is made by performing just one matrix inversion and the coupled model is directly obtained in a minimal-order form. However, it introduces the disadvantage of coupling a maximum of two substructures at same time. Furthermore, to compute the transformation matrix to transform a state-space model into coupling form the

choice of a subspace from a nullspace is required. This choice is hard to make and strongly affects the performance of the transformation [10]. Recently, a new coupling form that requires the computation of two nullspaces, but does not rely on the choice of any subspace was proposed in [14] and its performance will be also evaluated in this document.

Gibanica in [10] ported the technique developed by Sjövall and Abrahamsson in [12] into the general framework presented by de Klerk et al. [4]. By performing such porting operation, the limitation of coupling a maximum of two substructures at same time was eliminated, but two matrix inversions were now required to compute the coupled state-space model.

In an attempt to merge the advantages of each described SSS methods, Dias et al. in [9] developed the Lagrange Multiplier State-Space Substructuring (LM-SSS) method. This method just requires a single matrix inversion to compute the coupled state-space model, being able to couple several structures at same time. However, the LM-SSS approach requires a post-processing procedure to compute the minimal-order coupled state-space model and the elimination of the redundant DOFs from the obtained coupled state-space model.

The aim of this paper is to validate LM-SSS to couple and decouple state-space models, and to present a solution to retain the unique set of DOFs from the coupled state-space models without relying on a manual elimination. Moreover, the paper also presents a new and simpler coupling form that just requires the computation of a nullspace and does not rely on the choice of a subspace from the computed nullspace. The suitability of LM-SSS to couple state-space models established in modal domain previously transformed into coupling form in order to compute minimal-order coupled state-space models is also evaluated.

The LM-SSS method is described in section 3, while the procedure to perform decoupling is presented in section 4. Section 5 presents a solution to retain the unique set of DOFs from the coupled state-space model. Then, in sections 6 and 7 a new coupling form is introduced and the procedure to eliminate redundant states which are originated from coupling and decoupling operations is discussed, respectively. Afterwards, in section 8 the performance of LM-SSS to couple and decouple state-space models established in modal domain is evaluated and discussed by using a numerical example. Finally, the conclusions are presented in section 9.

2. Nomenclature

For easier understanding of all the parameters used in this article, the nomenclature is given in table 1.

3. Lagrange Multiplier State-Space Substructuring

The Lagrange Multiplier State-Space Substructuring is a novel SSS method introduced in [9]. To get a short insight into the approach, let us consider the assembled structure shown in figure 1.

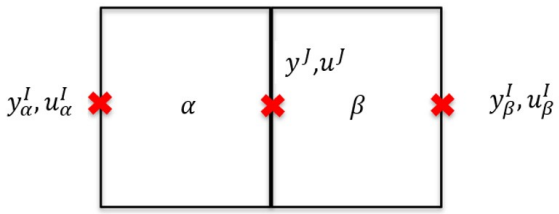

Figure 1: Assembled structure composed by two different components [9].

LM-SSS relies on the construction of a diagonal coupled state-space model. This model is obtained by writing the state-space matrices of each substructure to be coupled in block diagonal form and by using the forces that are responsible to keep the substructures coupled, which are usually tagged as connecting forces. When the substructures are coupled (see figure 1) the connecting forces that are acting at their interfaces are mutually cancelled, since they are equal in intensity and opposite in direction. However, if these substructures are virtually separated, we may observe the connecting forces acting at the interface of each component as depicted in figure 2.

As $\{g^J_\alpha(t)\} = -\{g^J_\beta(t)\}$, we may use the mapping matrix presented by de Klerk et al. in [6] in order to obtain a more compact representation for the relation between both connecting forces:

Table 1: Nomenclature

A	state matrix	M	mass matrix
B	input matrix	N	nullspace of a matrix
B_M	mapping matrix	q	state vector written in modal coordinates
C	output matrix	T	transformation matrix
D	feed-through matrix	u	input vector
g	connecting forces vector	V	damping matrix
H	FRF matrix	x	state vector
K	stiffness matrix	y	output vector
L	Boolean localization matrix	z	state vector transformed into coupling form
γ	Gaussian distributed independent stochastic variable	λ	Lagrange multipliers vector
θ	Gaussian distributed independent stochastic variable	μ	residual difference
$\bullet_{accel}$	acceleration state-space model	$\bullet_j$	j:th input
$\bullet_D$	block diagonal matrix	$\bullet_k$	k:th discrete frequency
$\bullet_{disp}$	displacement state-space model	$\bullet_S$	S:th substructure
$\bullet_i$	i:th output	$\bullet_{vel}$	velocity state-space model
$\bullet_\alpha$	substructure α	$\bullet_\beta$	substructure β
$\bullet^{-1}$	inverse of a matrix	$\bullet^\dagger$	pseudoinverse of a matrix
$\bullet^I$	internal DOF	$\bullet^T$	transpose of a vector/matrix
$\bullet^J$	interface DOF		
$\dot{\bullet}$	first order time derivative	$\ddot{\bullet}$	second order time derivative
$\bar{\bullet}$	coupling vector/matrix	$\widetilde{\bullet}$	vector composed by the unique set of DOFs

$$\begin{Bmatrix} \{g_\alpha(t)\} \\ \{g_\beta(t)\} \end{Bmatrix} = -[B_M]^T \{\lambda(t)\} \tag{1}$$

where, $\{\lambda(t)\}$ is the vector of Lagrange Multipliers that represent connecting forces [6] and $[B_M]$ represents the signed Boolean mapping matrix. Note that, this matrix is presented as $[B]$ matrix in [6], but here will be denoted as $[B_M]$ to avoid confusion with the $[B]$ state-space matrix. The vectors $\{g_\alpha(t)\}$ and $\{g_\beta(t)\}$ are given as follows.

$$\{g_\alpha(t)\} = \begin{Bmatrix} \{0\} \\ \{g_\alpha^J(t)\} \end{Bmatrix} \tag{2a}$$

$$\{g_\beta(t)\} = \begin{Bmatrix} \{0\} \\ \{g_\beta^J(t)\} \end{Bmatrix} \tag{2b}$$

Considering figure 2 and equation (1) and generalizing for coupling an unlimited number of structures, a diagonal coupled state-space model can be constructed as follows

$$\begin{aligned} \begin{Bmatrix} \{\dot{x}_\alpha(t)\} \\ \{\dot{x}_\beta(t)\} \\ \vdots \end{Bmatrix} &= [A_D] \begin{Bmatrix} \{x_\alpha(t)\} \\ \{x_\beta(t)\} \\ \vdots \end{Bmatrix} + [B_D] \left(\begin{Bmatrix} \{u_\alpha(t)\} \\ \{u_\beta(t)\} \\ \vdots \end{Bmatrix} - [B_M]^T \begin{Bmatrix} \{\lambda_\alpha(t)\} \\ \{\lambda_\beta(t)\} \\ \vdots \end{Bmatrix} \right) \\ \begin{Bmatrix} \{\ddot{y}_\alpha(t)\} \\ \{\ddot{y}_\beta(t)\} \\ \vdots \end{Bmatrix} &= [C_{accel,D}] \begin{Bmatrix} \{x_\alpha(t)\} \\ \{x_\beta(t)\} \\ \vdots \end{Bmatrix} + [D_{accel,D}] \left(\begin{Bmatrix} \{u_\alpha(t)\} \\ \{u_\beta(t)\} \\ \vdots \end{Bmatrix} - [B_M]^T \begin{Bmatrix} \{\lambda_\alpha(t)\} \\ \{\lambda_\beta(t)\} \\ \vdots \end{Bmatrix} \right) \end{aligned} \tag{3}$$

where,

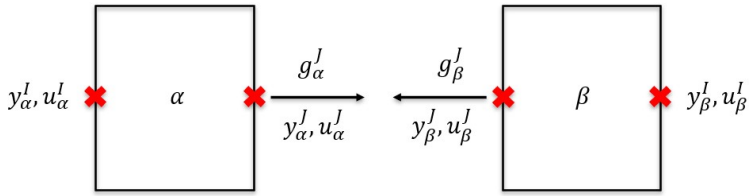

Figure 2: Components virtually separated [9].

$$
\begin{aligned}
[A_D] &= \begin{bmatrix} A_\alpha & & \\ & A_\beta & \\ & & \ddots \end{bmatrix}, \quad [B_D] = \begin{bmatrix} B_\alpha & & \\ & B_\beta & \\ & & \ddots \end{bmatrix} \\
[C_{accel,D}] &= \begin{bmatrix} C_{accel,\alpha} & & \\ & C_{accel,\beta} & \\ & & \ddots \end{bmatrix}, \quad [D_{accel,D}] = \begin{bmatrix} D_{accel,\alpha} & & \\ & D_{accel,\beta} & \\ & & \ddots \end{bmatrix}
\end{aligned} \tag{4}
$$

$\{x(t)\} \in \mathbb{R}^{n\times 1}$ represents the state vector, $\{u(t)\} \in \mathbb{R}^{n_i\times 1}$ represents the input vector, whose elements are forces and $\{\ddot{y}(t)\} \in \mathbb{R}^{n_o\times 1}$ represents the acceleration output vector. Subscripts α and β denote variables related to substructures α and β, respectively. Subscript *accel* denotes a state-space matrix of an acceleration state-space model (state-space model whose output vector elements are accelerations), while subscript D denotes a block diagonal matrix.

By using a more compact representation, the diagonal coupled state-space model (equation (3)) can be rewritten as follows:

$$
\begin{aligned}
\{\dot{x}(t)\} &= [A_D]\{x(t)\} + [B_D](\{u(t)\} - [B_M]^T\{\lambda(t)\}) \\
\{\ddot{y}(t)\} &= [C_{accel,D}]\{x(t)\} + [D_{accel,D}](\{u(t)\} - [B_M]^T\{\lambda(t)\})
\end{aligned} \tag{5}
$$

When substructures are coupled, they must verify continuity at their interface. This condition can be mathematically represented by using the mapping matrix $[B_M]$ as follows:

$$
[B_M]\{y(t)\} = \{0\} \tag{6}
$$

Since we are working with state-space models whose outputs represent accelerations (acceleration state-space models), equation (6) must hold also for accelerations.

$$
[B_M]\{\ddot{y}(t)\} = \{0\} \tag{7}
$$

Besides the interface continuity requirement, coupled substructures must also verify the local equilibrium equations given by the output equations of the diagonal coupled state-space model (equation (5)). By solving these equations it is possible to find the value of $\{u(t)\}$:

$$
\{u(t)\} = [D_{accel,D}]^{-1}(\{\ddot{y}(t)\} - [C_{accel,D}]\{x(t)\}) + [B_M]^T\{\lambda(t)\} \tag{8}
$$

By using together equations (7) and (8), and dropping $\{\bullet\}$, $[\bullet]$ and (t) for ease of readability, we can write these equations as given below:

$$
\begin{cases}
(D_{accel,D})^{-1}(\ddot{y} - C_{accel,D}x) + B_M^T\lambda = u \\
B_M\ddot{y} = 0
\end{cases} \tag{9}
$$

From the system of equations (9), the following relations can be obtained:

$$\begin{cases} \lambda = (B_M D_{accel,D} B_M^T)^{-1}(B_M C_{accel,D} x + B_M D_{accel,D} u) \\ \ddot{y} = (C_{accel,D} - D_{accel,D} B_M^T (B_M D_{accel,D} B_M^T)^{-1} B_M C_{accel,D}) x + (D_{accel,D} - D_{accel,D} B_M^T (B_M D_{accel,D} B_M^T)^{-1} B_M D_{accel,D}) u \end{cases} \tag{10}$$

By using equation (8) and the bottom equation of the system of equations (10), the state equations of the diagonal coupled state-space model (equation (5)) can be rewritten as follows:

$$\dot{x} = (A_D - B_D B_M^T (B_M D_{accel,D} B_M^T)^{-1} B_M C_{accel,D}) x + (B_D - B_D B_M^T (B_M D_{accel,D} B_M^T)^{-1} B_M D_{accel,D}) u \tag{11}$$

By using equation (11) and the bottom equation of the system of equations (10), the coupled state-space model is achieved as follows:

$$\begin{aligned} \{\dot{\bar{x}}(t)\} &= [\bar{A}]\{x(t)\} + [\bar{B}]\{\bar{u}(t)\} \\ \{\ddot{\bar{y}}(t)\} &= [\bar{C}_{accel}]\{\bar{x}(t)\} + [\bar{D}_{accel}]\{\bar{u}(t)\} \end{aligned} \tag{12}$$

where,

$$\begin{aligned} [\bar{A}] &= A_D - B_D B_M^T (B_M D_{accel,D} B_M^T)^{-1} B_M C_{accel,D} \\ [\bar{B}] &= B_D - B_D B_M^T (B_M D_{accel,D} B_M^T)^{-1} B_M D_{accel,D} \\ [\bar{C}_{accel}] &= C_{accel,D} - D_{accel,D} B_M^T (B_M D_{accel,D} B_M^T)^{-1} B_M C_{accel,D} \\ [\bar{D}_{accel}] &= D_{accel,D} - D_{accel,D} B_M^T (B_M D_{accel,D} B_M^T)^{-1} B_M D_{accel,D} \end{aligned} \tag{13}$$

overbar variables represent variables of the coupled state-space model.

At this point, is important to mention that several system identification methods developed to estimate state-space models from FRFs provide an estimation of the displacement state-space model (see for example [15]). However, to deduce LM-SSS technique we have used acceleration state-space models, hence this SSS technique has been established just to couple this kind of models. Thus, in general the estimated state-space models must be double differentiated in order to obtain the respective acceleration model.

By double differentiating a generic displacement state-space model, the respective acceleration state-space model is obtained as follows [16]:

$$\begin{aligned} \{\dot{x}(t)\} &= [A]\{x(t)\} + [B]\{u(t)\} \\ \{\ddot{y}(t)\} &= [C_{disp}AA]\{x(t)\} + ([D_{disp}] + [C_{disp}AB])\{u(t)\} \end{aligned} \tag{14}$$

Observing equation (14), we conclude that the acceleration state-space matrices can be calculated from the displacement ones as follows:

$$[A_{accel}] = \Big[A\Big], \quad [B_{accel}] = \Big[B\Big], \quad [C_{accel}] = \Big[C_{disp}AA\Big] \quad [D_{accel}] = \Big[C_{disp}AB\Big] + [D_{disp}] \tag{15}$$

By using the expressions in equation (15), we may rewrite equations (13) as follows:

$$\begin{aligned} [\bar{A}] &= A_D - B_D B_M^T (B_M (C_{disp,D} A_D B_D) B_M^T)^{-1} B_M (C_{disp,D} A_D A_D) \\ [\bar{B}] &= B_D - B_D B_M^T (B_M (C_{disp,D} A_D B_D) B_M^T)^{-1} B_M (C_{disp,D} A_D B_D) \\ [\bar{C}_{accel}] &= C_{disp,D} A_D A_D - (C_{disp,D} A_D B_D) B_M^T (B_M (C_{disp,D} A_D B_D) B_M^T)^{-1} B_M (C_{disp,D} A_D A_D) \\ [\bar{D}_{accel}] &= C_{disp,D} A_D B_D - (C_{disp,D} A_D B_D) B_M^T (B_M (C_{disp,D} A_D B_D) B_M^T)^{-1} B_M (C_{disp,D} A_D B_D) \end{aligned} \tag{16}$$

By using expressions (15), equation (16) can be rewritten in order to directly provide the coupled displacement state-space model:

$$
\begin{aligned}
[\bar{A}] &= A_D - B_D B_M^T (B_M (C_{disp,D} A_D B_D) B_M^T)^{-1} B_M (C_{disp,D} A_D A_D) \\
[\bar{B}] &= B_D - B_D B_M^T (B_M (C_{disp,D} A_D B_D) B_M^T)^{-1} B_M (C_{disp,D} A_D B_D) \\
[\bar{C}_{disp}] &= C_{disp,D} - (C_{disp,D} A_D B_D) B_M^T (B_M (C_{disp,D} A_D B_D) B_M^T)^{-1} B_M (C_{disp,D}) \\
[\bar{D}_{disp}] &= C_{disp,D} A_D B_D - (C_{disp,D} A_D B_D) B_M^T (B_M (C_{disp,D} A_D B_D) B_M^T)^{-1} B_M (C_{disp,D} A_D B_D) - \bar{C}_{disp} \bar{A} \bar{B} = 0
\end{aligned}
\tag{17}
$$

To define an expression to directly compute the coupled velocity state-space model (state-space model whose output vector elements are velocities), let us start analyzing how the state-space matrices of this model can be obtained from the respective displacement ones. By differentiating a generic displacement state-space model, we obtain the following velocity model [16]:

$$
\begin{aligned}
\{\dot{x}(t)\} &= [A]\{x(t)\} + [B]\{u(t)\} \\
\{\dot{y}(t)\} &= [C_{disp} A]\{x(t)\} + ([D_{disp}] + [C_{disp} B])\{u(t)\}
\end{aligned}
\tag{18}
$$

By using expressions (14) and (18), the following relations to compute the velocity state-space matrices form the acceleration ones can be established:

$$
[A_{vel}] = \left[A_{accel}\right], \quad [B_{vel}] = \left[B_{accel}\right], \quad [C_{vel}] = \left[C_{accel} A^{-1}\right] \quad [D_{vel}] = \left[D_{accel} A^{-1}\right] \tag{19}
$$

By using expression (19), expression (16) can be rewritten to directly compute the coupled velocity state-space model as follows:

$$
\begin{aligned}
[\bar{A}] &= A_D - B_D B_M^T (B_M (C_{disp,D} A_D B_D) B_M^T)^{-1} B_M (C_{disp,D} A_D A_D) \\
[\bar{B}] &= B_D - B_D B_M^T (B_M (C_{disp,D} A_D B_D) B_M^T)^{-1} B_M (C_{disp,D} A_D B_D) \\
[\bar{C}_{vel}] &= C_{disp,D} A_D - (C_{disp,D} A_D B_D) B_M^T (B_M (C_{disp,D} A_D B_D) B_M^T)^{-1} B_M (C_{disp,D} A_D) \\
[\bar{D}_{vel}] &= C_{disp,D} B_D - (C_{disp,D} A_D B_D) B_M^T (B_M (C_{disp,D} A_D B_D) B_M^T)^{-1} B_M (C_{disp,D} B_D)
\end{aligned}
\tag{20}
$$

where, subscrip *vel* denotes a state-space matrix of a velocity state-space model. If the coupled state-space model respects the second law of Newton $[C_{disp,D} B_D] = [0]$ [16],[12], hence $[\bar{D}_{vel}] = [0]$.

4. Decoupling

Decoupling is used to identify the dynamic behaviour of a component that is part of an assembled structure. This approach can only be applied if the dynamic behaviour of the assembled structure and of the remaining components is known. By using decoupling we may benefit from several advantages, for instance, having the possibility to dynamically characterize parts that are difficult to be tested separately [17] (such as rubber mounts [18],[19]).

To decouple a substructure we may use the Inverse Coupling approach [20],[17]. This decoupling procedure follows the same methodology as coupling. However, the state-space model of the substructure to be decoupled must be established in negative form [13],[20]. Then from the obtained state-space model, the inputs and outputs of the substructure to be characterized must be retained while the others must be eliminated. This is equivalent to just keep the columns of the input and feed-through matrices that are being multiplied by the inputs of the substructure to be identified and keep the rows of the output and feed-through matrices correspondent to the outputs of the same substructure.

The negative form of a state-space model can be derived by using a numerical state-space model. This kind of models can be directly computed from the mass, stiffness and damping matrices of the mechanical system being analyzed [10]. Let us consider the following acceleration state-space model:

$$
\begin{aligned}
\{\dot{x}(t)\} &= [A]\{x(t)\} + [B]\{u(t)\} \\
\{\ddot{y}(t)\} &= [C]\{x(t)\} + [D]\{u(t)\}
\end{aligned}
\tag{21}
$$

where, the state-space matrices are given as follows:

$$[A] = \begin{bmatrix} -M^{-1}V & -M^{-1}K \\ I & 0 \end{bmatrix}, \quad [B] = \begin{bmatrix} M^{-1} \\ 0 \end{bmatrix}$$
$$[C] = \begin{bmatrix} -M^{-1}V & -M^{-1}K \end{bmatrix}, \quad [D] = \begin{bmatrix} M^{-1} \end{bmatrix} \tag{22}$$

matrices $[M]$, $[K]$ and $[V]$ are the mass, stiffness and damping matrices respectively.

The computation of the negative form of the state-space model given by expression (21) can be performed by multiplying the matrices $[M]$, $[K]$ and $[V]$ by -1 [13],[20], as follows:

$$[A] = \begin{bmatrix} -(-M)^{-1}(-V) & -(-M)^{-1}(-K) \\ I & 0 \end{bmatrix}, \quad [B] = \begin{bmatrix} -M^{-1} \\ 0 \end{bmatrix}$$
$$[C] = [-(-M)^{-1}(-V) \quad -(-M)^{-1}(-K)], \quad [D] = \begin{bmatrix} -M^{-1} \end{bmatrix} \tag{23}$$

By observing the state-space matrices given by expression (23), one realizes that to obtain the negative form of an acceleration state-space model, its input and feed-through matrices must be multiplied by -1, whereas the remaining ones do not go through any mathematical operation. Even though, the computation of the negative form of a state-space model was demonstrated for a theoretical model, this procedure continues to be valid when working with state-space models established in modal domain.

5. Retaining the unique set of interface DOFs

When coupling by using LM-SSS the full set of interface DOFs is retained. Hence, for each pair of connected DOFs, two outputs and inputs with the same physical meaning will be present on the coupled state-space model. The elimination of these repeated inputs and outputs can be easily achieved by eliminating one of the correspondent columns of the $[B]$ and $[D]$ matrices and one of the correspondent rows of the $[C]$ and $[D]$ matrices, respectively [9]. However, when several DOFs are being coupled this procedure might get cumbersome, which may lead to erroneous eliminations.

To easily eliminate the redundant inputs and outputs, the relations between the full sets and unique sets of inputs and outputs will be used. Those relations were established in [4] by using a Boolean localization matrix $[L]$, which can be computed from the nullspace of the mapping matrix $[B_M]$. These relations are given as follows:

$$\{\widetilde{u}(t)\} = [L]^T\{u(t)\} \tag{24a}$$

$$\{y(t)\} = [L]\{\widetilde{y}(t)\} \tag{24b}$$

where, $\{\widetilde{u}(t)\}$ represents the unique set of force inputs and $\{\widetilde{y}(t)\}$ represents the unique set of displacements outputs.

Consider now a generic acceleration coupled state-space model obtained by using the LM-SSS method:

$$\begin{aligned} \{\dot{\bar{x}}(t)\} &= [\bar{A}]\{\bar{x}(t)\} + [\bar{B}]\{\bar{u}(t)\} \\ \{\ddot{\bar{y}}(t)\} &= [\bar{C}]\{\bar{x}(t)\} + [\bar{D}]\{\bar{u}(t)\} \end{aligned} \tag{25}$$

Since the state-space model used here to demonstrate the retention of the unique set of DOFs by using the $[L]$ matrix presents accelerations as outputs, the second order time derivative of equation (24b) must be computed as follows:

$$\{\ddot{y}(t)\} = [L]\{\ddot{\widetilde{y}}(t)\} \tag{26}$$

By using equations (24a) and (26), expression (25) can be rewritten as follows:

$$\begin{aligned} \{\dot{\bar{x}}(t)\} &= [\bar{A}]\{\bar{x}(t)\} + [\bar{B}]([L]^T)^{\dagger}\{\widetilde{u}(t)\} \\ [L]\{\ddot{\widetilde{y}}(t)\} &= [\bar{C}]\{\bar{x}(t)\} + [\bar{D}]([L]^T)^{\dagger}\{\widetilde{u}(t)\} \end{aligned} \tag{27}$$

where, superscript † represents the pseudoinverse of a matrix.

By using the Moore-Penrose pseudoinverse of matrix $[L]$, the output equation of the state-space model given by expression (27) can be rewritten as follows:

$$\begin{aligned} \{\dot{\bar{x}}(t)\} &= [\bar{A}]\{\bar{x}(t)\} + [\bar{B}]([L]^T)^\dagger\{\widetilde{u}(t)\} \\ \{\ddot{\widetilde{y}}(t)\} &= [L]^\dagger[\bar{C}]\{\bar{x}(t)\} + [L]^\dagger[\bar{D}]([L]^T)^\dagger\{\widetilde{u}(t)\} \end{aligned} \tag{28}$$

Equation (28) represents the state-space model given by expression (25) composed by a unique set of interface inputs and outputs, hence without the presence of redundant inputs and outputs.

It is worth mentioning that since $[L]$ is Boolean it will represent an orthogonal basis of the nullspace of the mapping matrix $[B_M]$. Hence, the computation of $[L]^\dagger$ and $([L]^T)^\dagger$ will be computationally efficient, because the matrix to be inverted is diagonal [9],[21].

6. Unconstrained Coupling Form

As referred in section 1, when coupling state-space models established in modal domain, they must be previously transformed into coupling form in order to get to a minimal-order coupled state-space model. The same statement is valid for the decoupling operation. Hence, this procedure will equally promote the presence of redundant states on the obtained model representative of the substructure to be identified.

A general state vector transformation into coupling form is given as follows [12]:

$$\{z_\alpha(t)\} = [T_\alpha]\{q_\alpha(t)\} = \begin{Bmatrix} \dot{y}_\alpha^J \\ y_\alpha^J \\ x_\alpha^I \end{Bmatrix} \tag{29}$$

where, $[T] \in \mathbb{R}^{n\times n}$ is the matrix responsible for transforming a state-space model into coupling form, $\{q(t)\} \in \mathbb{R}^{n\times 1}$ represents a state vector written in modal domain and $\{z(t)\} \in \mathbb{R}^{n\times 1}$ represents a state vector transformed into coupling form. Superscripts I and J denote variables related to internal and interface DOFs, respectively.

A general construction of the $[T_\alpha]$ matrix can be described as follows:

$$[T_\alpha] = \begin{Bmatrix} C_{disp,\alpha}^J A_\alpha \\ C_{disp,\alpha}^J \\ N_\alpha \end{Bmatrix} \tag{30}$$

where, the first block row transforms the states into the first derivative of the output DOFs and the second block row transforms the states into the output DOFs [16]. The last block row represented by $N_\alpha \in \mathbb{R}^{n-2n_J\times n}$ performs a transformation of the internal states and is included to ensure that the dimension of the state-space matrices are kept.

Conversely to the SSS method presented in [12], LM-SSS couples all the states of the state-space models to be coupled. Hence, the internal states are not kept uncoupled. Therefore, the computation of $[N_\alpha]$ does not need to guarantee that the contribution of the interface inputs to the response of the transformed internal states is null. Consequently, the transformation applied to the internal states can be arbitrary, provided that $[T_\alpha]$ is full rank and invertible. The simplest procedure to calculate $[N_\alpha]$ in order to fulfill this requirement is given as follows:

$$\begin{bmatrix} C_{disp,\alpha}^J A_\alpha \\ C_{disp,\alpha}^J \end{bmatrix} [N_\alpha]^T = 0 \tag{31}$$

Equation (31) will always guarantee that $[T_\alpha]$ is full rank (see equation (30)), if $[C_{disp,\alpha}]$ is full row rank. This equation also concludes the development of a new coupling form specially tailored for LM-SSS. Due to its simplicity and for giving almost completely freedom for the transformation of the internal states, this coupling form will be labelled as Unconstrained Coupling Form (UCF).

When compared with the coupling form developed in [12], UCF holds the advantage of not relying on the selection of a subspace from a nullspace. The selection of this subspace is difficult and strongly influences the obtained results [10]. If UCF is compared with the coupling form presented in [14] it has the advantage of just requiring the computation of one nullspace.

Note that, before transforming a general state-space model into coupling form, its input and output vectors must be partitioned in terms of interface and internal DOFs, and rearranged as follows.

$$\{u_\alpha(t)\} = \begin{Bmatrix} u_\alpha^J(t) \\ u_\alpha^I(t) \end{Bmatrix} \tag{32a}$$

$$\{y_\alpha(t)\} = \begin{Bmatrix} y_\alpha^J(t) \\ y_\alpha^I(t) \end{Bmatrix} \tag{32b}$$

The state-space matrices must be rearranged in accordance with the input and output vectors.

7. Minimal-order coupled state-space models

Unlike the SSS method proposed in [12], when coupling state-space models previously transformed into coupling form LM-SSS is not able to directly compute a minimal-order coupled state-space model [9]. However, since these models were transformed into coupling form, the state vector will contain the interface outputs and respective first derivatives of each substructure, being possible to perform the elimination of the redundant states. Thus, the computation of minimal-order coupled state-space models is still possible.

To better demonstrate how the redundant states must be eliminated, let us assume that the substructures represented in figure 1 were coupled by using LM-SSS. Hence, the state vector of the computed coupled state-space model would be given as follows:

$$\{\bar{z}(t)\} = \left\{ \dot{\bar{y}}_\alpha^J(t) \quad \bar{y}_\alpha^J(t) \quad \bar{x}_\alpha^I(t) \quad \dot{\bar{y}}_\beta^J(t) \quad \bar{y}_\beta^J(t) \quad \bar{x}_\beta^I(t) \right\}^T \tag{33}$$

During the coupling procedure, compatibility is enforced at the interface of the substructures to be coupled (see section 3), thus we have the following equalities.

$$\{\bar{y}^J\} = \{\bar{y}_\alpha^J\} = \{\bar{y}_\beta^J\} \tag{34a}$$

$$\{\dot{\bar{y}}^J\} = \{\dot{\bar{y}}_\alpha^J\} = \{\dot{\bar{y}}_\beta^J\} \tag{34b}$$

By observing expressions (33), (34a) and (34b), we conclude that to obtain the minimal realization of the computed coupled state-space model, $\{\bar{y}_\alpha^J\}$ or $\{\bar{y}_\beta^J\}$ must be kept while the other vector must be eliminated from the coupled state-space model. The same is valid for the respective first order derivatives. These state eliminations cannot be performed by simply removing one state of each pair of states that present the same physical meaning. Even though the states to be eliminated are redundant, their contribution for the dynamics of the coupled system is not null. Thus, their impact over the dynamics of the assembled structure must be retrieved by the states that are kept on the model. To properly perform these eliminations is suggested the use of the post-processing procedures outlined in [9].

It is worth noticing that the procedures here presented and discussed to eliminate the redundant states originated from coupling are still valid and can be applied in a similar way to eliminate the redundant states originated from a decoupling operation.

8. Numerical Example

The approaches discussed in the previous sections will be demonstrated hereafter by adopting a numerical example. The dynamic system synthesized is represented by the two components shown in figure 3. The assembled structure obtained when both components are coupled is presented in figure 4, being the values of the physical parameters indicated in both figures given in table 2.

Firstly, the estimation of state-space models from the FRFs of components *A* and *B* is performed. Then, to validate UCF presented in section 6, the identified state-space models will be transformed into this coupling form and into the ones presented in [12] and [14]. The FRFs of the untransformed and of the three transformed identified models of each component are then compared (section 8.1).

In section 8.2, the coupling of the identified state-space models will be performed by using the LM-SSS method (see section 3), being the FRFs of the coupled model compared with the ones of the exact model and with the coupled FRFs obtained by applying LM FBS [6] to couple the FRFs of the identified models. To validate LM-SSS to compute minimal-order models, this SSS technique will be applied to compute coupled models from the identified models transformed into different coupling forms, being the elimination of the redundant states present on those coupled

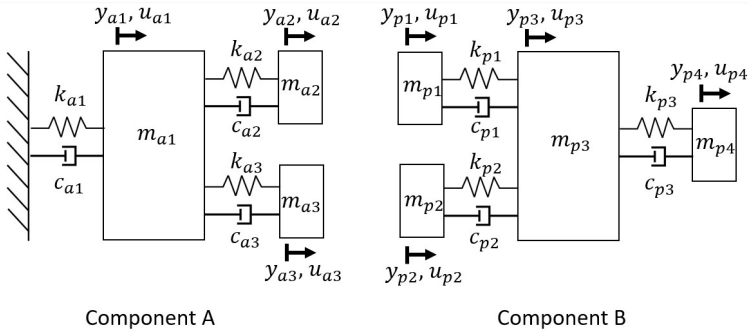

Figure 3: Uncoupled components.

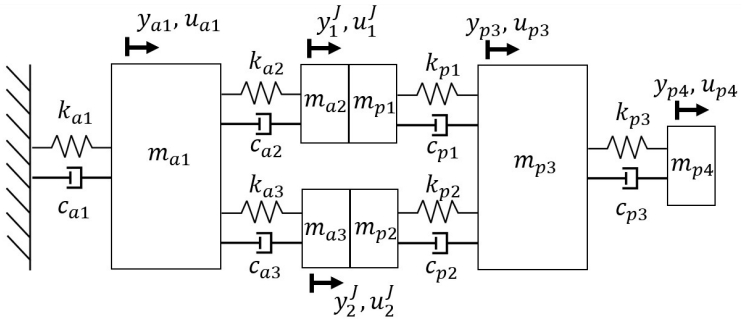

Figure 4: Assembled system.

models performed by following the procedures described in section 7. The FRFs of the computed minimal-order models will be, then, compared with the ones of the coupled model computed from the untransformed identified models.

Finally, in section 8.3 LM-SSS will be evaluated to perform decoupling in order to identify the state-space model of the component *B*. Then, the FRFs of the obtained model will be compared with the FRFs of the exact model and the FRFs of the model identified by using the system identification method and with the FRFs obtained by using LM FBS decoupling. To demonstrate that the procedures described in section 7 are valid to eliminate redundant states originated from a decoupling operation, the identification of the state-space model of component *B* will be repeated by using state-space models previously transformed into coupling form. The FRFs of the obtained models are then compared with the FRFs of the model obtained from LM-SSS decoupling by using untransformed state-space models.

8.1. Identified State-Space Models

The computation of the exact state-space model of the components and of the assembled system was performed by using its mass, stiffness and damping matrices in accordance with equations (21) and (22). The mass and stiffness matrices were established by using the Lagrange equations [22], while for simplicity the damping matrix of each substructure was constructed from the respective stiffness one by replacing the stiffness terms with the damping ones.

To approximate the numerical example under study to an experimental one, artificial noise was introduced into the FRFs of both components. The computation of the perturbed FRFs was performed by following the procedure used in [12]. This procedure perturbs the real and imaginary parts of each element of the FRFs according to equation (35).

$$H_{S,ij}(\omega_k) = H_{S,ij}(\omega_k) + \gamma_{ijk} + j\theta_{ijk} \tag{35}$$

where, subscript S denotes the substructure to which the FRFs that are being perturbed belong, while subscripts i, j and k denote the output, input and the discrete frequency of the FRF term that is being perturbed. Variables γ and θ are Gaussian distributed independent stochastic variables with zero mean and a standard deviation, for the specific case, assumed to be equal to $5 \times 10^{-3}\ ms^{-2}N^{-1}$.

Table 2: Physical parameter values

i	m_i (kg)	c_i (Nsm^{-1})	k_i (Nm^{-1})
$a1$	10	30	1.5×10^5
$a2$	3	50	5×10^5
$a3$	3	50	4.5×10^5
$p1$	5	50	1×10^5
$p2$	7	50	1.5×10^5
$p3$	10	10	5×10^3
$p4$	1	-	-

To identify state-space models from the computed noisy FRFs, the polyreference least-squares complex frequency domain method (PolyMAX) [23] and the Maximum Likelihood Modal Parameter method (ML-MM) [24] were applied to estimate the modal parameters from the noisy FRFs. Then, these identified parameters were used to construct the respective state-space models. The comparison of a noisy FRF with the FRF of the exact model and the FRF of the identified model for component A is given in figure 5, while the same comparison for component B is shown in figure 6.

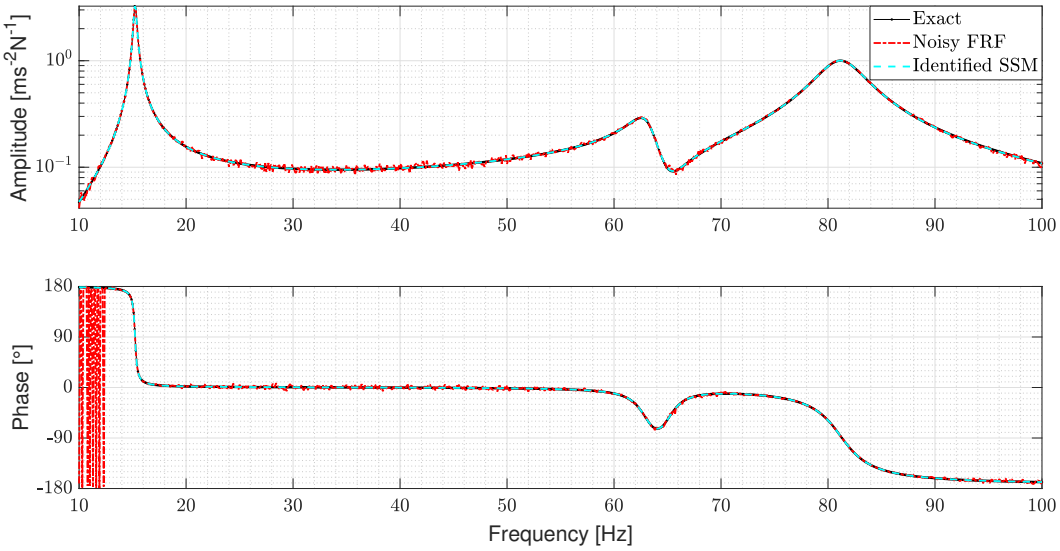

Figure 5: Accelerance FRF of the component A, whose output is the DOF $a3$ and the input is the DOF $a1$.

Afterwards, the identified state-space models were transformed into the coupling forms presented in [12] (from now on labelled as OCF, standing for Original Coupling Form) and [14] (from now on labelled as NOCF, standing for New Original Coupling Form) and into UCF presented in section 6. In figures 7 and 8 the comparison of one FRF of the identified untransformed model and of the same model transformed into different coupling forms is shown for components A and B respectively.

By analyzing figures 5 and 6 it is evident that the system identification method used was able to filter-out the artificial noise introduced on the FRFs of both components, thus leading to an accurate identification of the state-space models of both components (the identified models of components A and B were composed by $n_A = 18$ and $n_B = 22$ states, respectively). However, it was found that the state-space models were not passive. Looking at figures 7 and 8, it is well evident that for both the components the FRF of the identified transformed models into OCF and

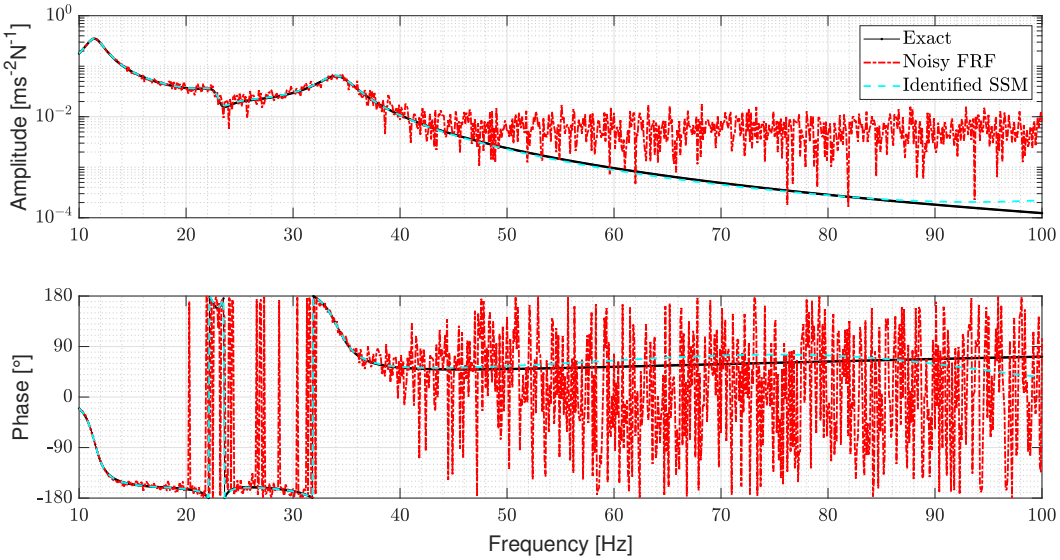

Figure 6: Accelerance FRF of the component B, whose output is the DOF $p4$ and the input is the DOF $p1$.

UCF is very well matching the one of the untransformed model. Hence, we may conclude that the transformation of both identified state-space models into these two different coupling forms was successfully performed. However, it was found that the transformation into NOCF lead to poor results. This poor performance might be explained by its transformation matrix being close to be singular. Indeed, as proven in Appendix A, we have no guarantee that the NOCF transformation matrix will be always well-conditioned and full rank. For the other coupling forms this is not verified. Provided that the input and output state-space matrices of the state-space model to be transformed are full column rank and full row rank, respectively [20], by using OCF we have freedom to select a subspace from the computed nullspace that makes the computation of a full rank transformation matrix possible [12]. Whereas, by using UCF, if the output state-space matrix of the state-space model to be transformed is full row rank, the transformation matrix will always be full rank as presented in section 6.

Note that, due to the poor performance of NOCF transformation, from now on the performance of UCF will be just compared with the one of OCF.

8.2. Coupling Results

In a first instance, the LM-SSS method was used to couple the untransformed identified state-space models. The obtained model presented $n_A + n_B = 40$ states as expected. To compute this coupled model, the retention of the unique set of DOFs was performed by following the procedure outlined in section 5. Then, the coupling was made by using LM FBS to couple the FRFs of the identified state-space models. Figure 9 shows the comparison of a coupled FRF obtained by using LM FBS method with the same FRF of the exact assembled state-space model and of the non minimal-order coupled model.

By analyzing figure 9, it is evident that the FRF of the exact assembled model and the FRF of the non minimal-order coupled model are well matching. Furthermore, the FRF computed from LM FBS perfectly matches the one of the coupled state-space model. However, the coupled state-space model was found to be unstable, presenting five real positive poles. The presence of those non-physical poles might be a consequence of the non-passivity of the identified state-space models [12].

To evaluate the performance of LM-SSS to compute minimal-order models by coupling state-space models previously transformed into coupling form and by using the procedures described in section 7, LM-SSS was applied to compute minimal-order coupled models (it was found that these models presented $n_A + n_B - 2n_J = 36$ states as expected) from the identified models transformed into two different coupling forms (OCF and UCF). For ease of implementation, the retention of the unique set of DOFs of the computed coupled state-space models was performed

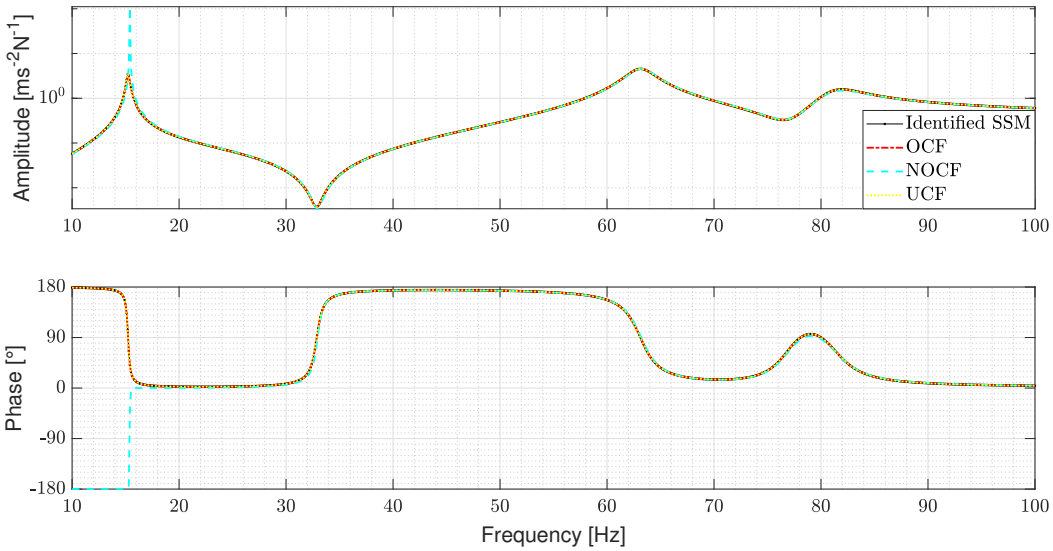

Figure 7: Accelerance FRF of the component A, whose output is the DOF $a3$ and the input is the DOF $a3$.

by following the procedure outlined in section 5. For the same reason, the post-processing procedure presented in [9] that relies on the use of a Boolean localization matrix $[L_T]$ was used to eliminate the redundant states. Figure 10 shows the comparison between the FRF of the non-minimal order coupled model and the three FRFs obtained by the different minimal order models.

Figure 10 proves that LM-SSS and the procedures described in section 7 to obtain minimal order coupled models are consistent. For the two different minimal-order coupled state-space models were found three non-physical poles (i.e. real positive poles), which might be a direct consequence of the transformed identified state-space models not be passive, as pointed out in [12]. The decrease of the number of non-physical poles, when compared with the non-minimal order coupled model is a consequence of the elimination of the redundant states. This verification highlights the importance of removing these spurious states from the coupled state-space models.

8.3. Decoupling Results

To validate LM-SSS to perform decoupling, this method was applied to decouple the identified state-space model of component A (see section 8.1) from the non minimal-order coupled state-space model computed in section 8.2. The same procedure was performed by decoupling from the FRFs of the non minimal-order coupled model the identified FRFs of component A by using the LM FBS technique.

Figure 11 shows the comparison of the identified FRF of component B by using LM FBS-based decoupling and the same FRF of the exact model as well as the FRF of the model identified in section 8.1 and the FRF of the model identified by performing LM-SSS-based decoupling. It is well evident that the FRFs of the identified model of component B are well matching the FRF of the exact model. Furthermore, the identified FRF obtained by using LM FBS-based decoupling and the one of the identified model of component B obtained in section 8.1 are perfectly fitting the one of the identified model obtained by applying LM-SSS-based decoupling. Hence, we may claim that LM-SSS technique is validated to perform decoupling.

At this point, we are interested in demonstrating that LM-SSS is able to decouple state-space models previously transformed into coupling form and that by using the procedures described in section 7 we may eliminate from the identified model the redundant states, whose presence is due to the decoupling operation. To perform this demonstration, the identification of a state-space model for component B was performed by decoupling the identified model of A previously transformed into different coupling forms from the minimal order coupled state-space models (which are already obtained in coupling form) computed in section 8.2.

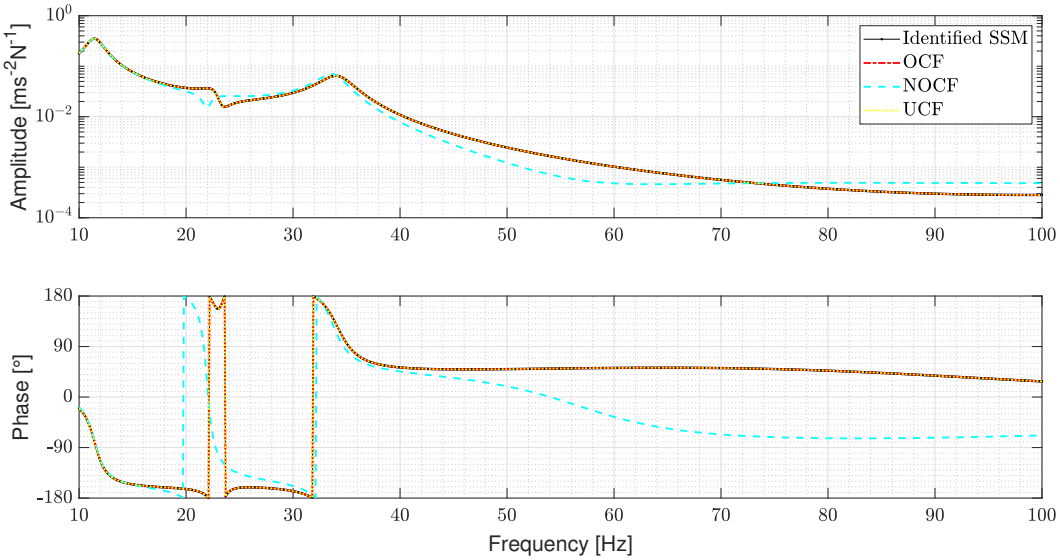

Figure 8: Accelerance FRF of the component B, whose output is the DOF $p1$ and the input is the DOF $p4$.

In figure 12 a comparison of a FRF of the identified state-space model of component B by using untransformed models and by using models transformed into different coupling forms is presented. By observing this figure, we may conclude that the FRFs of both identified models are very well matching, validating LM-SSS to decouple state-space models previously transformed into coupling form and the procedures described in section 7 to eliminate the redundant states, whose origin is a consequence of the decoupling operation.

As final analysis, it is worth discussing on the number of states of the identified models of component B by using decoupling. The state-space model obtained by using untransformed models presented $n_A + n_B + n_A = 58$ states, while the one obtained by using models transformed into coupling form presented $n_A + n_B - 2n_J + n_A - 2n_J = 50$ states, being found that all the state-space models presented several unstable poles. It is evident that these models present more states than the identified state-space model obtained from the system identification routines. Hence, the identified models by using LM-SSS decoupling are non minimal-order models. This may explain, together with the lack of passivity of the used state-space models, the presence of unstable poles.

The verified increment of states is a consequence of the inclusion of the dynamics of the component A into the coupled model in order to perform its decoupling (see section 4). Hence, the dynamics of this component will be present twice on the identified model, since it was already included in the coupled model. Due to the double presence of the dynamics of component A, pairs of spurious modes will be present on the identified model [20]. Distinguishing spurious modes from physical ones might be hard to accomplish, especially, if there is no previous knowledge about the structure to be identified, which is a common situation. Thus, if possible, it is recommended to avoid decoupling operation by using system identification methods to identify state-space models from the FRFs of the components.

9. Conclusion

The LM-SSS method showed to be reliable to couple and decouple state-space models established in modal domain. It has been demonstrated that the method is able to couple and decouple state-space models transformed into coupling form and to perform the elimination of the redundant states originated from coupling and decoupling operations by using post-processing procedures. It was also shown that the FRFs of the coupled models calculated by LM-SSS are exactly the same as the coupled FRFs obtained by using LM FBS method [6] (see section 8.2). The same applies for the decoupling operation (see section 8.3).

Furthermore, due to the LM-SSS coupling formulation it was possible to establish a new coupling form, denoted unconstrained coupling form (see section 6). This coupling form holds the advantage of just requiring the computation

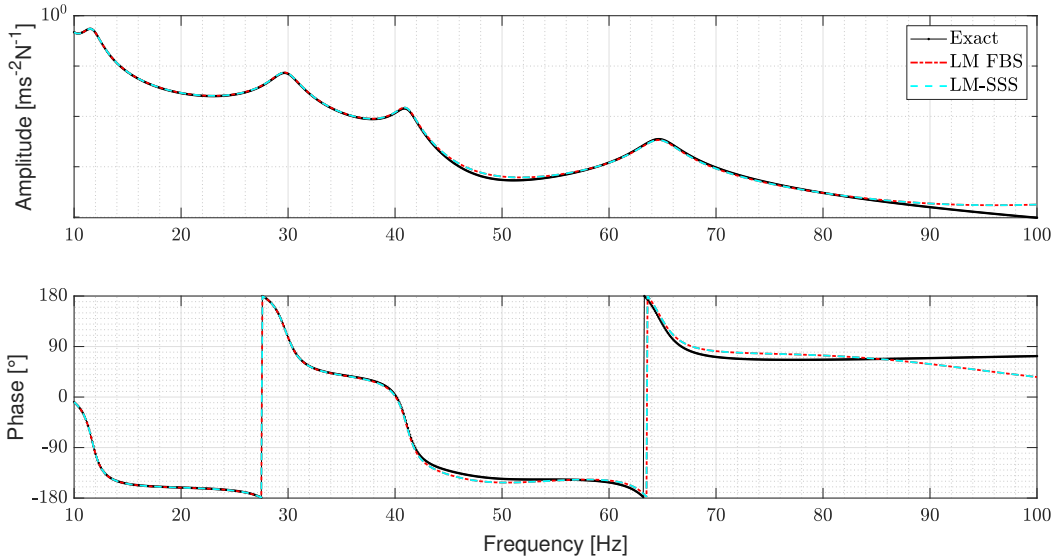

Figure 9: Accelerance FRF of the coupled system, whose output is the interface DOF $p4$ and the input is the interface DOF 1.

of a nullspace and does not rely on the choice of a subspace from the computed nullspace. The performance of UCF showed to be similar to the coupling forms already available to the scientific community (see sections 8.1, 8.2 and 8.3).

Credit authorship contribution statement

R.S.O. Dias: Conceptualization, Investigation, Methodology, Software, Formal analysis, Validation, Data curation, Writing - original draft, Writing - review & editing. **M. Martarelli**: Conceptualization, Methodology, Resources, Funding Acquisition, Writing - review & editing, Supervision, Project administration. **P. Chiariotti**: Conceptualization, Methodology, Resources, Funding Acquisition, Writing - review & editing, Supervision, Project administration.

Declaration of Competing Interest

The authors declare that they have no known competing financial interests or personal relationships that could have appeared to influence the work reported in this paper.

Acknowledgements

The authors gratefully acknowledge Dr. Mahmoud El-Khafafy from Siemens Industry Software NV for supporting the research by providing the system identification algorithm to estimate state-space models from FRFs.

Funding

This project has received funding from the European Union's Framework Programme for Research and Innovation Horizon 2020 (2014-2020) under the Marie Sklodowska-Curie Grant Agreement nº 858018.

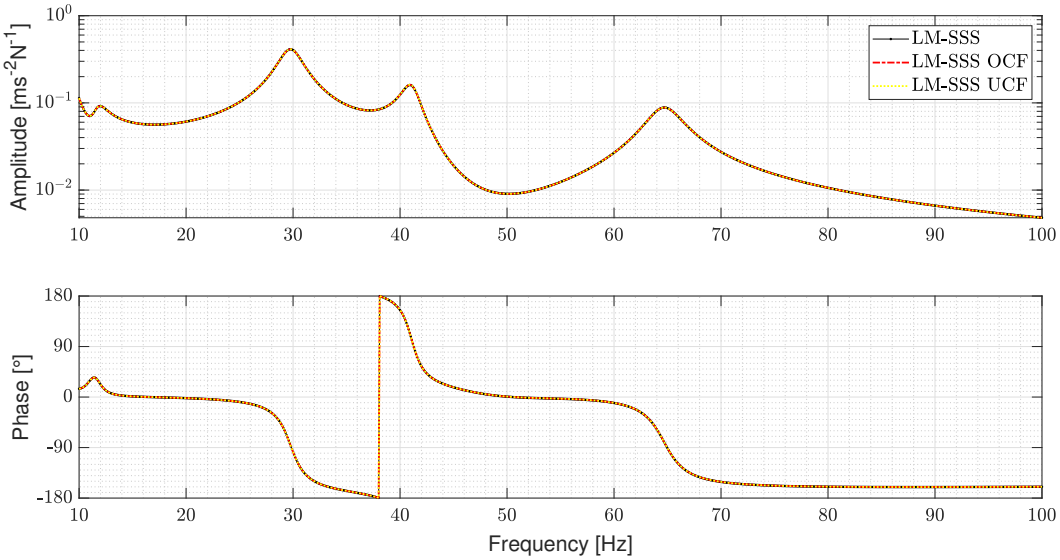

Figure 10: Accelerance FRF of the coupled system, whose output is the interface DOF 1 and the input is the DOF $p3$.

Appendix A. New Original Coupling Form

In this section, the coupling form presented in [14] will be deduced and analyzed in order to demonstrate that there is no guarantee that its transformation matrix will be full rank. Hence, there exists the possibility that the computed transformation matrix be singular, which would lead to ill-conditioned state vector transformations.

A general transformation matrix to transform a state vector into coupling form is given as follows [12]:

$$[T_{NOCF}] = \begin{bmatrix} C^J_{disp}A \\ C^J_{disp} \\ N \end{bmatrix} \tag{A.1}$$

where, $N \in \mathbb{R}^{n-2n_J \times n}$.

Let us introduce nullspaces $N_B \in \mathbb{R}^{n-n_J \times n}$ and $N_C \in \mathbb{R}^{n-2n_J \times n}$ that are given as follows:

$$[N_B][B^J] = \{0\} \tag{A.2a}$$

$$\begin{bmatrix} C^J_{disp}A \\ C^J_{disp} \end{bmatrix} [N_C]^T = \{0\} \tag{A.2b}$$

where, superscripts J denote quantities associated to interface DOFs.

To avoid numerical problems during the performance of such state transformation, $[T_{NOCF}]$ must be invertible and, hence full rank. To make sure that this matrix will be full rank independently of the state-space model under study (provided that its input and output matrices are full column rank and full row rank, respectively), the following relation must be verified:

$$\begin{bmatrix} C^J_{disp}A \\ C^J_{disp} \end{bmatrix} \begin{bmatrix} N \end{bmatrix}^T = \begin{bmatrix} 0 \end{bmatrix} \tag{A.3}$$

At this point, we immediately understand that $[N] = [N_C]$ would be a perfect choice to make sure that the relation established in equation (A.3) is fulfilled (such choice would lead to UCF presented in section 6). However, as previously mentioned, the coupling technique presented in [12] requires that $[N]$ is also a nullspace of $[B^J]$, which is a condition not necessarily verified by $[N_C]$. Thus, the problem can be posed as follows:

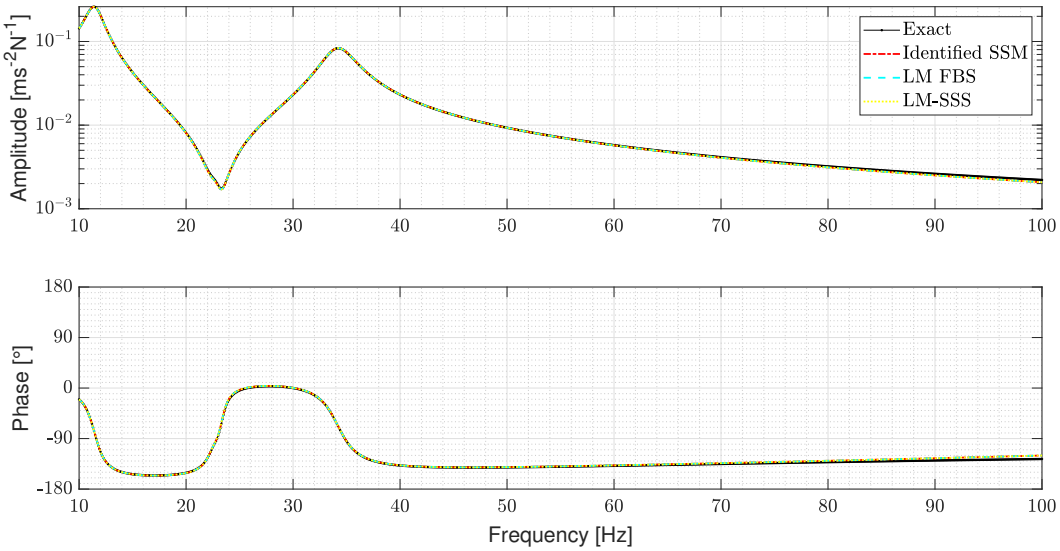

Figure 11: Accelerance FRF of the component B, whose output is the DOF $p3$ and the input is the DOF $p4$.

$$N = N_A N_B = N_C \tag{A.4}$$

where, $[N_A]$ is a matrix that is intended to be calculated so that $[N_A][N_B]$ is as close as possible to $[N_C]$. The calculation of $[N_A]$ is therefore a suitable task for least-squares. The computation of this solution can be performed by simply inverting $[N_B]$ [25], resulting in the following expression:

$$N_A = N_C N_B^{\dagger} \tag{A.5}$$

where, superscript † represents the pseudoinverse of a matrix.

Since $[N_B]$ is the left nullspace of $[B^J]$, $[N_B]$ is full row rank and its pseudoinverse can be calculated as follows [21]:

$$N_B^{\dagger} = N_B^T (N_B N_B^T)^{-1} \tag{A.6}$$

where, $[N_B]^{\dagger}$ works as right inverse of $[N_B]$, hence $[N_B][N_B]^{\dagger} = [I]$.

By using equation (A.6) , equation (A.5) can be rewritten as follows:

$$N_A = N_C N_B^T (N_B N_B^T)^{-1} \tag{A.7}$$

By using equations (A.4) and (A.7), an expression to calculate $[N]$ can be outlined as given below:

$$N = N_C N_B^T (N_B N_B^T)^{-1} N_B \tag{A.8}$$

Due to the use of least-squares to compute $[N]$, equality (A.4) is usually not true, being verified a residual difference between $[N_C]$ and $[N]$:

$$\mu = N_C - N_C N_B^T (N_B N_B^T)^{-1} N_B = N_C - N_C N_B^{\dagger} N_B \tag{A.9}$$

where, $[N_B]^{\dagger}[N_B] \neq [I]$, since as previously mentioned $[N_B]^{\dagger}$ acts as the right inverse of $[N_B]$. Hence, there is the possibility of this residual difference to invalidate the equality presented in equation (A.3), which could promote the construction of a $[T_{NOCF}]$ matrix that is not full rank and, thus not invertible.

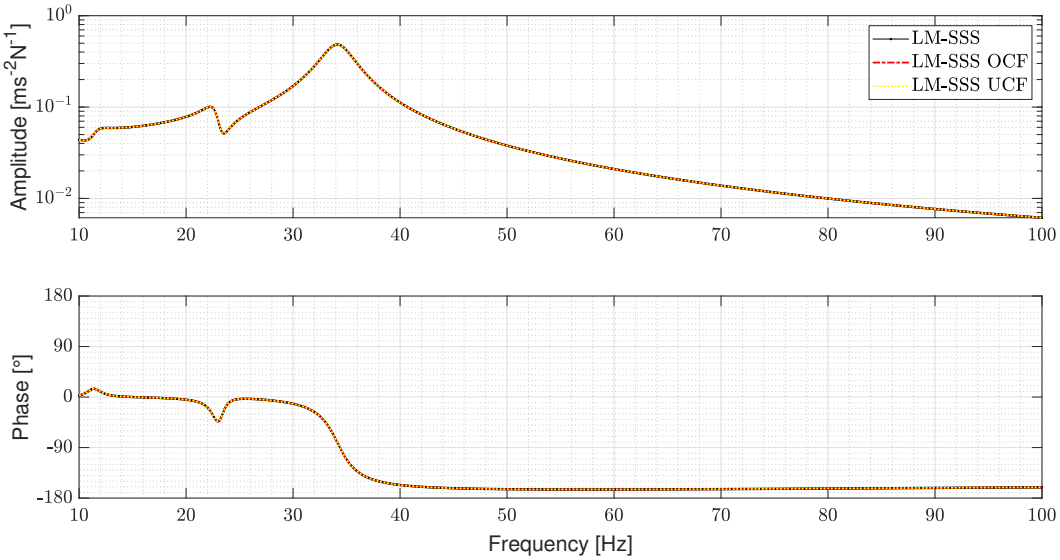

Figure 12: Accelerance FRF of the component B, whose output is the DOF $p1$ and the input is the interface DOF $p3$.

Let us develop expression (A.3) in order to better understand how the residual difference given by equation (A.9) can foster the construction of a singular $[T_{NOCF}]$ matrix. By using equation (A.8) and the transpose property $(AB)^T = B^T A^T$ [25], $[N]^T$ may be established as follows:

$$N^T = N_B^T((N_B N_B^T)^{-1})^T N_B N_C^T \tag{A.10}$$

The combination of equation (A.10) and equation (A.3) leads to:

$$\begin{bmatrix} C_{disp}^J A N_B^T((N_B N_B^T)^{-1})^T N_B N_C^T \\ C_{disp}^J N_B^T((N_B N_B^T)^{-1})^T N_B N_C^T \end{bmatrix} = \begin{bmatrix} 0 \end{bmatrix} \tag{A.11}$$

Assuming that $[N_B]$ is calculated to be an orthonormal basis for the nullspace of $[B^J]$, which is a common practice, $[N_B][N_B]^T = [I]$ [25] and the following relation can be established:

$$((N_B N_B^T)^{-1})^T = (N_B N_B^T)^{-1} \tag{A.12}$$

By using equations (A.6) and (A.12), equation (A.11) can be rewritten as follows:

$$\begin{bmatrix} C_{disp}^J A N_B^\dagger N_B N_C^T \\ C_{disp}^J N_B^\dagger N_B N_C^T \end{bmatrix} = \begin{bmatrix} 0 \end{bmatrix} \tag{A.13}$$

Equality (A.13) may not be verified, because $[N_B]^\dagger[N_B] \neq [I]$. Hence, we may conclude that $[N]$ will not necessarily verify expression (A.3), being impossible to guarantee that $[T_{NOCF}]$ will be full rank, independently of the state-space model intended to be transformed.

References

[1] A. Mahmoudi, D. Rixen, C. Meyer, Comparison of Different Approaches to Include Connection Elements into Frequency-Based Substructuring, Experimental Techniques (2020). doi:10.1007/s40799-020-00360-1.

[2] R. Craig, M. Bampton, Coupling of substructures for dynamic analyses, AIAA Journal 6 (7) (1968) 1313–1319. URL https://doi.org/10.2514/3.4741

[3] D. Rixen, A dual Craig–Bampton method for dynamic substructuring, Journal of Computational and Applied Mathematics 168 (2004) 383–391.
URL https://doi.org/10.1016/j.cam.2003.12.014
[4] D. Klerk, D. Rixen, S. Voormeeren, General framework for dynamic substructuring: History, review, and classification of techniques, AIAA J. 46 (5) (2008) 1169–1181.
URL https://doi.org/10.2514/1.33274
[5] B. Jetmundsen, R. Bielawa, W. Flannelly, Generalized frequency domain substructure synthesis, Journal of the American Helicopter Society 33 (1988) 55–64.
[6] D. de Klerk, D. J. Rixen, J. de Jong, The frequency based substructuring (fbs) method reformulated according to the dual domain decomposition method, In: 24th International Modal Analysis Conference, St. Louis, MO (2006).
[7] D. Rixen, Substructuring using impulse response functions for impact analysis, In: Proceedings of the SEM IMAC - XXVIII Jacksonville, Florida, USA (2010). doi:10.1007/978-1-4419-9834-7_56.
[8] T.-J. Su, J.-N. Juang, Substructure system identification and synthesis, Journal of Guidance, Control and Dynamics 17 (5) (1994) 1087–1095.
[9] R. Dias, M. Martarelli, P. Chiariotti, Lagrange Multiplier State-Space Substructuring, Journal of Physics: Conference Series 2041 (1) (2021) 012016. doi:10.1088/1742-6596/2041/1/012016.
URL https://doi.org/10.1088/1742-6596/2041/1/012016
[10] M. Gibanica, Experimental-Analytical Dynamic Substructuring: a state-space approach, Master's Thesis, Chalmers University Technology, Götenborg, Sweden (2013).
[11] M. Gibanica, A. T. Johansson, A. Liljerehn, P. Sjövall, T. Abrahamsson, Experimental-analytical dynamic substructuring of ampair testbed: A state-space approach. In: M. Allen, R. Mayes, D.Rixen (eds) Dynamics of Coupled Structures, Conference Proceedings of the Society for Experimental Mechanics Series. Springer International Publishing. 1 (2014) 1–14.
URL https://doi.org/10.1007/978-3-319-04501-6_1
[12] P. Sjövall, T. Abrahamsson, Component system identification and state-space model synthesis, Mechanical Systems and Signal Processing 21 (2007) 2697–2714.
URL https://doi.org/10.1016/j.ymssp.2007.03.002
[13] M. Scheel, M. Gibanica, A. Nord, State-space dynamic substructuring with the transmission simulator method, Experimental Techniques 43 (2019) 325–340. doi:10.1007/s40799-019-00317-z.
URL https://doi.org/10.1007/s40799-019-00317-z
[14] M. Allen, D. Rixen, M. van der Seijs, P. Tiso, T. Abrahamsson, R. Mayes, Substructuring in Engineering Dynamics, Springer International Publishing, 2020.
[15] M. Gibanica, T. Abrahamsson, Identification of physically realistic state-space models for accurate component synthesis, Mechanical Systems and Signal Processing 145 (2020) 106906. doi:https://doi.org/10.1016/j.ymssp.2020.106906.
[16] F. Lembregts, J.Leuridan, H. V. Brussel, Frequency domain direct parameter identification for modal analysis: State space formulation, Mechanical Systems and Signal Processing 4 (1990) 65–75. doi:10.1016/0888-3270(90)90041-I.
URL https://doi.org/10.1016/0888-3270(90)90041-I
[17] W. D'Ambrogio, A. Fregolent, Direct hybrid formulation for substructure decoupling, In: In: R. Mayes et al. (eds) Topics in Experimental Dynamics Substructuring and Wind Turbine Dynamics, Volume 2. Conference Proceedings of the Society for Experimental Mechanics Series. Springer, New York (2012). doi:10.1007/978-1-4614-2422-2_11.
URL https://doi.org/10.1007/978-1-4614-2422-2_11
[18] M. Haeussler, S. Klaassen, D. Rixen, Experimental twelve degree of freedom rubber isolator models for use in substructuring assemblies, Journal of Sound and Vibration 474 (2020) 115253.
URL https://doi.org/10.1016/j.jsv.2020.115253
[19] J. O. Almirón, F. Bianciardi, P. Corbeels, R. Ullmann, W. Desmet, Mount characterization analysis in the context of fbs for component-based tpa on a wiper system, Forum Acusticum 2020, Lyon, France (2020). doi:10.48465/fa.2020.0251.
[20] M. Scheel, State-Space Experimental-Analytical Dynamic Substructuring Using the Transmission Simulator, Master's Thesis, Chalmers University Technology, Götenborg, Sweden (2015).
[21] M. A. M. Lasso, Linear vector space derivation of new expressions for the pseudo inverse of rectangular matrices, Journal of Applied Research and Technology 5 (3) (2007) 150–159.
URL https://doi.org/10.22201/icat.16656423.2007.5.03.528
[22] H. Harrison, T. Nettleton, Advanced Engineering Dynamics, 1st edition Edition, Butterworth-Heinemann, 1997.
[23] B. Peeters, H. V. der Auweraer, P. Guillaume, J. Leuridan, The polymax frequency-domain method: a new standard for modal parameter estimation?, Schock and Vibration 11 (2004) 395–409.
[24] M. El-Kafafy, B. Peeters, P. Guillaume, T. D. Troyer, Constrained maximum likelihood modal parameter identification applied to structural dynamics, Mechanical Systems and Signal Processing 72-73 (2016) 567–589.
URL http://dx.doi.org/10.1016/j.ymssp.2015.10.030
[25] H. Anton, C. Rorres, Elementary linear algebra : applications version, 11th Edition, WILEY, 2013.